



Gelation of aqueous gelatin solutions. I. Structural investigation

Madeleine Djabourov, Jacques Leblond, Pierre Papon

► To cite this version:

Madeleine Djabourov, Jacques Leblond, Pierre Papon. Gelation of aqueous gelatin solutions. I. Structural investigation. Journal de Physique, 1988, 49 (2), pp.319-332. 10.1051/jphys:01988004902031900 . jpa-00210699

HAL Id: jpa-00210699

<https://hal.science/jpa-00210699>

Submitted on 4 Feb 2008

HAL is a multi-disciplinary open access archive for the deposit and dissemination of scientific research documents, whether they are published or not. The documents may come from teaching and research institutions in France or abroad, or from public or private research centers.

L'archive ouverte pluridisciplinaire **HAL**, est destinée au dépôt et à la diffusion de documents scientifiques de niveau recherche, publiés ou non, émanant des établissements d'enseignement et de recherche français ou étrangers, des laboratoires publics ou privés.

Classification

Physics Abstracts

82.70 — 07.60F — 61.40

Gelation of aqueous gelatin solutions. I. Structural investigation

Madeleine Djabourov, Jacques Leblond and Pierre Papon

Laboratoire de Physique Thermique (*), ESPCI, 10, rue Vauquelin, 75231 Paris Cedex 05, France

(Reçu le 25 juin 1987, accepté le 23 octobre 1987)

Résumé. — Nous avons étudié les modifications structurales des solutions de gélatine pour différents traitements thermiques et différentes concentrations. La structure est explorée à plusieurs échelles microscopiques, comprenant la transformation conformationnelle pelote \rightleftharpoons hélice des chaînes protéiques (par polarimétrie) et l'organisation supramoléculaire du réseau (par microscopie électronique). Le rôle du solvant dans le processus de gélification est révélé à l'aide de la résonance magnétique nucléaire du proton. Le non-équilibre de la phase gel est clairement mis en évidence, ainsi que son désordre topologique. Nous proposons une analyse phénoménologique de la cinétique de croissance des hélices, suivie d'une tentative de modélisation des mécanismes microscopiques s'appuyant sur les données connues.

Abstract. — We have investigated the structural modifications of aqueous gelatin solutions for various thermal treatments and different concentrations. The structure is explored at different microscopic levels, putting into evidence the conformational coil \rightleftharpoons helix transition of the proteic chains (by optical rotation), the supramolecular structure of the network (by electron microscopy) and the role of solvent (by proton nuclear magnetic resonance). The non-equilibrium nature of the gel phase is demonstrated as well as its disordered character. A phenomenological analysis of the kinetics of helix formation is proposed, followed by an attempt for a microscopic modelling of the mechanisms, based on the data presently known.

The gelation of aqueous gelatin solutions is a process which has been widely investigated in the past because of its important applications [1, 2].

In the last decade, the subject has regained a new stimulation arising both from the modern ideas on the gelation phenomenon, derived from the models of percolation and the scaling concepts — and from refined experimental facilities.

Starting with low concentrations, half a percent, and rising up to 50 %, the gelatin + water solutions form homogeneous systems which gel by lowering the temperature below 30 °C, say roughly at room temperature.

Gelatin is a biopolymer: it is a protein: it is denaturated collagen.

Due to the remarkable mechanical properties of the gels and to the natural biological origin of gelatin, the gels have been used for long in pharmacology, food, cosmetic applications, but also in quite different fields, such as photography, glues, composite materials.

Understanding the gelation process of this biomaterial is a quite delicate problem. Many factors are known to affect the properties of the gels: the ionic force, the pH of the solution, the molecular weight, the concentration, the origin of collagen itself...

However, for all the systems, the gelation mechanism is basically related to the change of only one thermodynamical parameter: temperature.

Clearly, gelation is a thermal effect. The gels are thermoreversible.

This work is mainly concerned with the influence of temperature on the structural and rheological parameters of the gelling solutions. Our aim is to elucidate the mechanisms of gelation in moderately concentrated solutions ($c \sim$ a few percent), to determine the most relevant structural parameters of the network and to relate them to the rheological measurements.

The phenomenological behaviour of the process is investigated.

From a more general point of view, gelation for gelatin gels is a physical process: whether it can be analysed within the same theoretical framework as

(*) Unité associée au Centre National de la Recherche Scientifique UA 836.

chemical gelation — i.e. using scaling laws — is an open question. We have tried also to answer to this question taking gelatin as an example.

We shall deal with the subject in two parts : the first one — this paper — is devoted to the structural investigation and to the microscopic mechanisms which are involved ; in the second part, we examine the rheological modifications during gelation, in relation with a critical phenomenon.

We start by recalling the main results on collagen and gelatin, at a molecular level, which are needed for explaining the mechanism of gelation. Then we present our experimental investigation, using mainly optical rotation methods and some proton nuclear magnetic resonance measurements. Observations of the gel network structure obtained by electron microscopy are also reported.

The interpretation of the data contains first a phenomenological analysis of the kinetics of structural changes (helix growth), followed by a microscopic model which can explain the overall process.

Collagen and gelatin.

As we said, gelatin is denatured collagen. Collagen is the major component of skin, tendons, bones, etc...

The chemical composition of collagen varies with its origin. There are as many as twenty different amino-acids which enter the composition of collagen in variable proportions. However, for this protein sequences of $-(\text{Gly-X-Pro})-$ or $-(\text{Gly-X-Hypro})-$ are often repeated. As a general rule every three residue is Gly. As a typical composition, one can think of 33 % Gly, 21 % Pro + Hypro, 10 % Ala, and the rest (36 %) being composed of many other X amino-acids in small proportions. Gly is the smallest amino-acid as its lateral group is only one hydrogen atom, while Pro and Hypro, with rigid lateral pyrrolidine rings have important sterical hindrances. It has been established by Ramachandran [1] that the molecular composition of the protein, and mainly the distribution of Gly along the chain is responsible for the conformation of the protein in the native state. Indeed, the collagen unit is a rod of 300 nm length, made of three strands, each having a molecular weight of 100 000. Each strand is twisted into a left-handed helix of about 0.9 nm pitch and all three are wrapped into a super-right-handed helix with a pitch of approximately 8.6 nm (roughly ten times longer than the left-handed helix). The presence of Gly is required to allow the three polypeptide chains to come closely together, while the Pro and Hypro residues enhance rigidity. The latter also contributes to stabilize the structure by additional hydrogen bonds [3]. The gradual right handed twist of the individual strands allows the side groups of amino-acids, of variable sizes, to come into the structure. Thus the triple helix structure, with nearly the same

parameters, is observed in synthetic poly-tripeptides [4] of variable lengths like the $-(\text{Gly-Pro-Pro})_n-$ or $-(\text{Gly-Pro-Hypro})_n-$.

The poly-proline polypeptides in aqueous solutions adopt the poly-L-proline II conformation, which is a single left-handed helix almost identical to the collagen left-handed helix, while the poly-glycine polypeptides form insoluble crystals made of left-handed helices (poly-glycine II) aligned parallel to each other.

Collagen obviously achieves a compromise between these two structures, which is due to its molecular composition and to the requirements of its hydrogen-bond stabilization. So, the collagen triple helix is stabilized by interchain hydrogen bonds which are perpendicular to the chain axes. The hydrogen bonds can be of several types : either directly between CO and NH groups belonging to two adjacent backbones, or *via* water molecules bridging between two CO groups or between CO and NH groups. The type and the number of hydrogen bonds per helix turn is still debated [5]. Additional covalent crosslinks bind the chains together at both ends of the rods. In the tissues, the rods of triple helices are arranged in fibers. A characteristic shift of 67 nm between adjacent rows is observed. The overall structure is summarized in figure 1.

Gelatin is derived from collagen by hydrolytic degradation. Acidic and alkaline treatments are

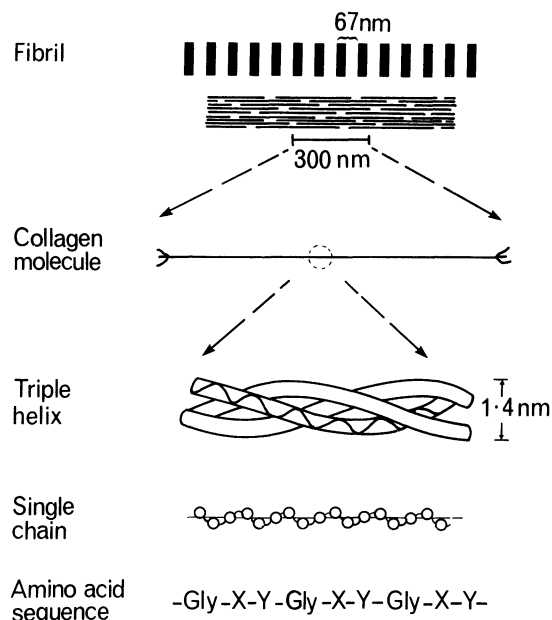


Fig. 1. — The structure of collagen molecules at different levels. From the top to the bottom : the typical striation of 67 nm of the collagen fibrils in native tissues, observed by electron microscopy ; the collagen rod triple helix ; the composition of a single chain, revealing the repetition of the sequence $-(\text{Gly-X-Y})-$, X and Y being different amino-acids (from Ref. [3]).

used in industrial processes [2]. The chemical treatment mainly breaks crosslinks between strands, but also may hydrolyse the strands into fragments. Thus a broad molecular weight distribution is obtained for gelatin.

In some cases, it is possible to extract the collagen rod without denaturing it [2]. Then it can be dissolved in acidic aqueous solutions. When the latter are heated, a helix \rightarrow coil transition is observed for the protein around 36 °C.

How do the gelatin gels form ?

Gelatin is easily dissolved in water by heating the solutions at about 40 to 50 °C.

Then the gelatin chains are believed to be in the coil conformation [6]. When solutions are cooled below 30 °C a reverse coil \rightarrow helix transition takes place which can be detected by important modifications of the optical rotation, mainly due to the left-handed helix conformation. As we said, helices have to be stabilized by hydrogen bonds which are perpendicular to their axes. Thus, at very low concentrations $c \sim 10^{-4}$ to 10^{-3} w/w intramolecular hydrogen bonds are formed preferentially by a back refolding of the single chains [7]. At higher concentrations, $c \geq 1$ % w/w, the helix growth induces chain association and three-dimensional network formation. Basically, two different models of chain association have been proposed :

- a conformational coil \rightarrow helix transition by local association of three different chains (inter-molecular bonds) along short helical sequences [7] ;

- a crystallization mechanism leading to fiber growth, similar to the fringed micelle model of synthetic polymers crystallization. The diameter of the fibers would depend on temperature and concentration [8].

We shall refer to these models further on in this paper.

The basic ideas concerning the molecular characteristics and the structure of collagen, as well as the mechanisms of gelation, being now introduced we can proceed with the experimental details of gel preparation and with the description of our investigations.

Sample characterization and gel preparation.

Our gelatin samples come from lime processed demineralized ossein, kindly provided by Société Rousselot (Isle-sur-Sorgue). The molecular characterization and purity analysis has been published previously [9]. The polydispersity is given by $\frac{\bar{M}_w}{\bar{M}_n} = 2.6$. The molecular weight distribution is well centred around $M_w = 100\,000$. Although the polydispersity is important it represents one of a high grade gelatin sample (photographic grade).

The sample preparation has also been described elsewhere [9].

The solvent is an aqueous solution 0.1 M NaCl. The pH was adjusted to 7 to avoid the isoelectric point (pH = 5).

The presence of NaCl fixes the ionic force of the solution and screens out the electrostatic interactions between the charged groups of the protein chains. A small amount of sodium azide is also added ; it prevents from bacterial contamination.

Experimental methods.

We use optical rotation measurements as a powerful method of detecting the conformational changes of the gelatin chains in solution. The optical rotation angle α is automatically measured with a Perkin Elmer 241 MC Polarimeter working at wavelengths $303 < \lambda < 579$ nm, with a precision of $\pm 0.001^\circ$. The cells have an optical path of 0.1 dm and a volume of 0.1 or 0.5 ml. Their temperature is controlled by an external bath circulating into the jacketed cells and measured with a thermocouple inserted into the cell, with an accuracy of ± 0.1 °C.

The proton NMR results, briefly recalled in this paper are obtained by using a Varian wide line spectrometer operating at 7.5 MHz and a pulsed BRUKER SXP-4-60 spectrometer operating at 15 and 40 MHz.

The sample preparation for electron microscopy observation is outlined in section 3.

1. Optical rotation of collagen solutions and gelatin gels.

1.1 THE METHOD. — In the ultraviolet or the visible range, protein solutions exhibit optical rotation effects which are due to electronic transitions involving delocalized π electrons of the peptide bond or of some lateral groups [10]. If the protein undergoes a coil \rightarrow helix transition, specific interactions between the peptide units appear, modifying the nature of the electronic transitions. The optical rotatory dispersion generally provides valuable information about possible conformations of the chains. Both the optical rotatory dispersion of native collagen in dilute solutions and of gelatin are known [11].

Native collagen exhibits a strong negative Cotton effect corresponding to an absorption band centred around

$$\lambda_0 = 210 \pm 5 \text{ nm}.$$

A similar behaviour is observed for poly-L-proline II solutions, meaning that the measurement is mainly sensitive to left-handed conformation of the single chains. The triple helix association gives a marginal distortion to the chains which seems to have little effect on the optical rotatory dispersion [12].

When the collagen solutions are denatured by heating, the amplitude of the Cotton effect decreases significantly, but λ_0 is almost constant.

Let $[\alpha]_\lambda$ be the specific rotation at a wave length defined by :

$$[\alpha]_\lambda = \frac{\alpha^{\text{meas.}}}{c \cdot l} \quad (1)$$

where $\alpha^{\text{meas.}}$ is the optical rotation angle, in degrees, c the concentration in g cm^{-3} , l the optical path of the cell in dm.

Von Hippel and Wong [13] have shown that at any wave length $\lambda > 300$ nm, the specific optical rotation of collagen or gelatin solutions can be analysed by using a Drude equation with a single term i.e. :

$$[\alpha]_\lambda = A \frac{\lambda_0^2}{\lambda^2 - \lambda_0^2} \quad (2)$$

The amplitude A depends on the conformation of the protein. Indeed, this relation stands also for partially renatured solutions [11].

As these relations have been rigorously established for rather dilute solutions, we have checked their validity for moderately concentrated solutions (a few percent) which correspond to the gel formation conditions.

In figure 2, we plot $[\alpha]^{-1}$ versus λ^2 for several temperatures, which correspond to the sol (hot solution, $T = 45^\circ\text{C}$) or the gel state ($T = 20^\circ\text{C}$, $T = 25^\circ\text{C}$, $T = 28^\circ\text{C}$). We also report the data for a native calf skin collagen solution in citric acid. Actually, one can see that the inverse of the specific optical rotation varies linearly with the of the wavelength, for $300 < \lambda < 579$ nm. All the lines converge to $\lambda_0 = 212$ nm, in agreement with the former observations. The lines are comprised between the two limiting values defined by the native collagen and the coil solutions. The slopes vary with the amount of helix renatured. By a homothetical transformation, the same information is derived from the measurements at any wavelength $\lambda > 300$ nm. This allows us to define a quantity which we call the helix amount χ , by :

$$\chi = \frac{[\alpha]_\lambda^{\text{meas.}} - [\alpha]_\lambda^{\text{coil}}}{[\alpha]_\lambda^{\text{collagen}} - [\alpha]_\lambda^{\text{coil}}} \quad (3)$$

χ is independent of λ , we assume that collagen is 100 % helix and that the hot solutions are completely denatured.

Further experiments are done at $\lambda = 436$ nm, corresponding to specific optical rotations :

$$\begin{aligned} [\alpha]_{436}^{\text{coil}} &= -256 \pm 5 \\ [\alpha]_{436}^{\text{collagen}} &= -800 \pm 10. \end{aligned}$$

The densities of the solutions are taken equal to lg. cm^{-3} .

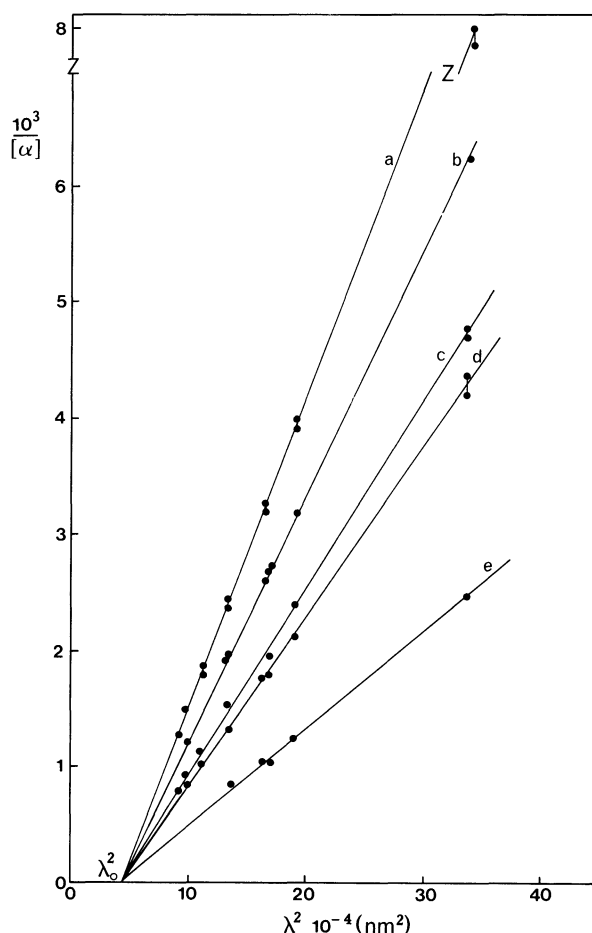


Fig. 2. — The inverse of the specific optical rotation, $[\alpha]$, versus the square of the wavelength, λ , in solutions and gels : a) gelatin solutions, $T = 45.5^\circ\text{C}$, $c = 1\%$ g/g ; and $c = 4.7\%$ g/g ; b) gel, $T = 28^\circ\text{C}$, $c = 4.7\%$ g/g ; c) gel, $T = 25^\circ\text{C}$, $c = 4.7\%$ g/g ; d) gel, $T = 20^\circ\text{C}$, $c = 1\%$ g/g ; e) native collagen solution, $T = 20^\circ\text{C}$, $c = 0.45\%$ g/g. $[\alpha]$ is defined in equation (1).

1.2 THERMAL TREATMENTS OF SOLUTIONS AND GELS. — We have tested different methods of preparing the gels : by lowering the temperature at constant rates, or by quenching the solutions at fixed temperatures.

1.2.1 Thermal cycles. — This method was used first. We reproduce in figure 3 the results from reference [14]. For three different rates of cooling v , $0.06 < v < 0.1^\circ\text{C/min}$, for a concentration $c = 4.6\%$ g/g, we lowered the temperature down to 4°C and then raised it back to 45°C .

Important hysteresis effects appear (width $\sim 6^\circ\text{C}$) although the curves do not show marked differences between the different rates. More helices are renatured at the lower rate of cooling, but the limiting value of 100 % helix is not reached. The hysteresis curves show the balance between the rate of helix growth or melting, and the rate of change of the temperature.

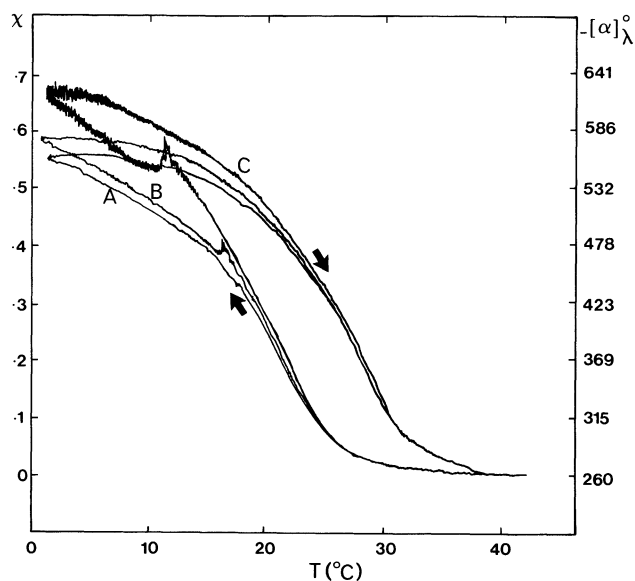


Fig. 3. — Hysteresis loops of gelatin solutions measured at $\lambda = 436$ nm, for three different rates of cooling and heating: A) $v = 0.1$ °C/min; B) $v = 0.08$ °C/min; C) $v = 0.06$ °C/min (concentration $c = 4.6$ %/g) (from Ref. [14]).

1.2.2 Quenching and annealing. — To better put into evidence these non-equilibrium effects, we preferred the method of quenching and annealing the gels for long periods (a hundred up to one thousand hours). Two different concentrations have been explored: 1 % g/g and 4.7 % g/g. Starting with hot solutions poured into the jacketed cells and stabilized at $T = 45$ °C, we quickly changed the thermostating liquid, by switching to a second bath regulated at a lower temperature (below 30 °C). The time for temperature equilibration is about two minutes. We automatically recorded the optical rotation angle as a function of time. In figure 4, we

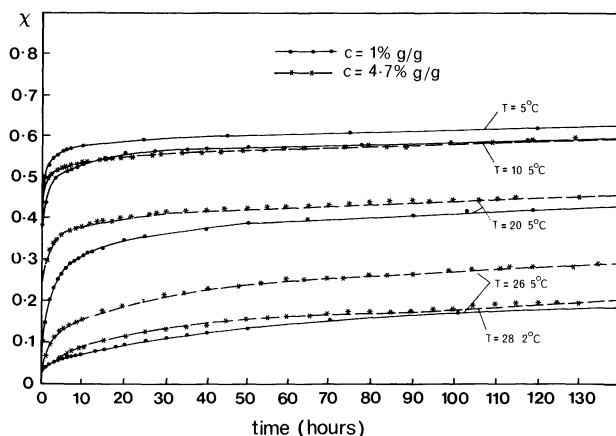


Fig. 4. — The increase of the helix amount *versus* time, in hours, for two concentrations and different quenching temperatures.

report the results concerning several temperatures and both concentrations. The time scale is given in hours. The kinetic behaviour is comparable for both concentrations. The following remarks can be done:

a) At the high temperatures, $T = 26.5$ °C and $T = 28.2$ °C, the helix amount χ increases progressively, but hardly reaches 20 to 25 % even after a very long period of annealing (140 h).

b) At intermediate temperatures $10 < T < 20$ °C, two different stages of the helix renaturation appear: a very rapid increase, which gives important amounts of helices (30-40 %) within less than one hour, followed by a smooth increase, which seems to lead towards an « final » value for χ .

c) At even lower temperatures, $5 < T < 10$ °C, the same trend appears, but although the helix amount is higher, a saturation effect is seen, around $\chi = 60$ -70 %.

d) Comparing both concentrations at the same temperature and at equal ages, we can see that the higher the concentration the higher the helix amount. The difference is noticeable at high temperatures and tends to disappear around 10 °C. The data are summarized in table I, for three different temperatures and for an annealing time $t = 100$ h.

Table I. — Helix amount reached after 100 h of annealing for two concentrations.

	$T = 26.5$ °C	$T = 20$ °C	$T = 10$ °C
$c = 1$ % g/g	$\chi = 0.175$	$\chi = 0.415$	$\chi = 0.585$
$c = 4.7$ % g/g	$\chi = 0.275$	$\chi = 0.445$	$\chi = 0.580$

1.2.3 Partial melting. — In these experiments, a gel which has been matured for a long period (260 h) at room temperature ($T = 20$ °C) was quickly brought to a higher temperature ($T = 28$ °C). Then, the experiment was repeated on the same sample, three other times, at a higher temperature each time. The optical rotation angle was recorded as previously. The final temperature did not exceed $T = 37$ °C, when all the helices would have disappeared. Thus we term these experiments the « partial melting » of the helices. We represent in figure 5 the helix amount as a function of time during the four consecutive steps. The time in abscissa is given in hours, on a logarithmic scale. This representation allows to display the process at short time scales (minutes) as well as at long time scales (hundred hours). We started with a helix amount $\chi = 0.48$, an initial temperature $T = 20$ °C and first raised the temperature to $T = 28$ °C. We can see in figure 5 that a great number of helices disappears in less than

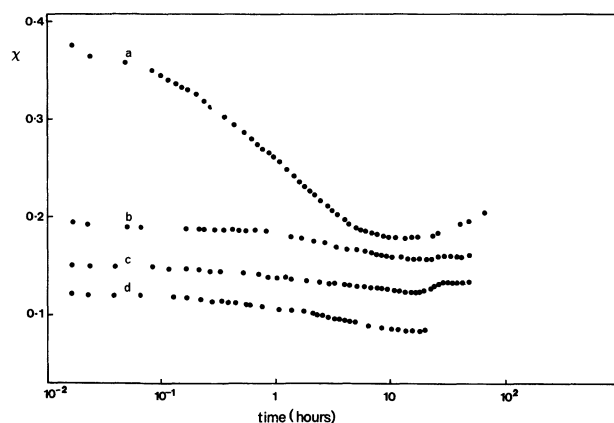


Fig. 5. — Partial melting of gels during four consecutive temperature jumps : a) gel matured for 260 h at $T = 20^\circ\text{C}$ then quenched at $T = 28^\circ\text{C}$; b) same experiment from $T = 28^\circ\text{C}$ to $T = 30^\circ\text{C}$; c) from $T = 30^\circ\text{C}$ to $T = 32^\circ\text{C}$; d) from $T = 32^\circ\text{C}$ to $T = 34^\circ\text{C}$ ($c = 4.7\%$ g/g).

10 min, the helix amount decreasing to $\chi = 0.30$. Then a much slower « melting » proceeds within 10 h leading to a minimum at $\chi = 0.18$, after which a slow increase can be seen again. After 80 h, we repeated a second heating step from $T = 28$ to $T = 30^\circ\text{C}$, during 50 h, followed by two other steps from $T = 30$ to $T = 32^\circ\text{C}$ (50 h), then from $T = 32$ to $T = 34^\circ\text{C}$ (24 h). Each time a similar behaviour is observed.

These experiments show that all the helices which were initially present do not have the same thermal stability. Few of them resist a temperature increase above 28°C , only 10 to 15 % of the helices are still present at higher temperatures ($30 \leq T \leq 34^\circ\text{C}$) and the growth of new ones is then considerably slowed down. « Stable » values of the helix amounts cannot be determined.

1.2.4 Complete melting. — In order to systematically study the thermal stability of gels formed in different thermal conditions, we adopt the method of progressively increasing the temperature at a constant rate. The optical rotation angle α was recorded as a function of the temperature up to 45°C (« complete melting »). We choose to study gels which have been formed and matured for long periods (120 to 150 h) at fixed temperatures (quenching experiments).

As we explained in the preceding sections, « equilibrium » melting curves of the gels are not available : at intermediate temperatures the growth of new helices is in competition with the melting of those formed at lower temperatures. We fixed the rate of temperature raise to $0.05^\circ\text{C}/\text{min}$ which is a high enough value for preventing growth of new helices but still sufficiently low to satisfy the thermal equilibrium and recording conditions.

The helix amount decreases as a function of temperature. The curves present a sigmoidal shape. The data (optical rotation angle) was stored on a Hewlett Packard plotter. A smoothing program was applied and the derivative $d\alpha/dT$ computed. The derivative is generally a peak centred around the inflexion point of $\alpha(T)$. The peak indicates the characteristic « melting » temperature of the helices. It contains essentially the same information as the endotherms measured by differential scanning calorimetry (DSC). In figure 6a, we plot the derivative α' versus T for gels of 1 % g/g concentration matured for 150 h at different temperatures $T = 5^\circ\text{C}$, $T = 10.5^\circ\text{C}$, $T = 20.5^\circ\text{C}$, $T = 26.5^\circ\text{C}$. The melting of a collagen dilute solution is also reported (at the same heating rate). Similar experiments were done on gels of 4.7 % g/g concentration and reported in figure 6b.

We are now able to compare the thermal stability of gels prepared in different conditions and we make the following statements :

a) For gels formed at $T \leq 20^\circ\text{C}$, the melting curve contains a single peak, which is centred on a variable temperature, T_m , which increases with the temperature, T_q , at which the gel was formed. For instance, $T_q = 5^\circ\text{C}$ and $T_m = 24.5^\circ\text{C}$, $T_q = 10^\circ\text{C}$ and $T_m = 25.5^\circ\text{C}$. Moreover the width of the peak is larger for gels formed at the lower temperatures. This indicates a wide spread of the thermal stability of the junctions which means a distribution of the size or of the degree of perfection of the structures inside the gel. This behaviour is particularly relevant for the gel formed at 5°C . The width of the peak is of 12°C and it is broader towards the lower temperatures. The gel formed at 10°C during 150 h has a slightly lower helix amount (see Fig. 4) but its thermal stability is improved ($T_m = 25.5^\circ\text{C}$, the width is of 9°C). This trend is confirmed for the higher temperatures of gelation.

b) The gels formed at $20 \leq T \leq 28^\circ\text{C}$ have a bimodal melting curve. The mean peak is shifted to temperatures above 30°C and a secondary peak appears centred around $T_m = 36^\circ\text{C}$. This second peak indicates the presence of a fraction having the thermal stability of collagen. This fraction increases, for increasing temperatures of gelation.

In order to summarize the results, we plot in figure 7 the melting temperatures as a function of the gelation temperature T_q , for both concentrations. The width of the peaks is represented by an error bar centred on the mean melting temperature T_m . T_m is a linear increasing function of T_q which can be extrapolated to the melting temperature of collagen for a gel ideally formed at 36°C . However for the highest gelation temperatures ($T_q = 26.5$ and $T_q = 28.2^\circ\text{C}$), the thermal stability is actually improved as compared with the extrapolation line. The bimodal behaviour is observed. We also reported in the same

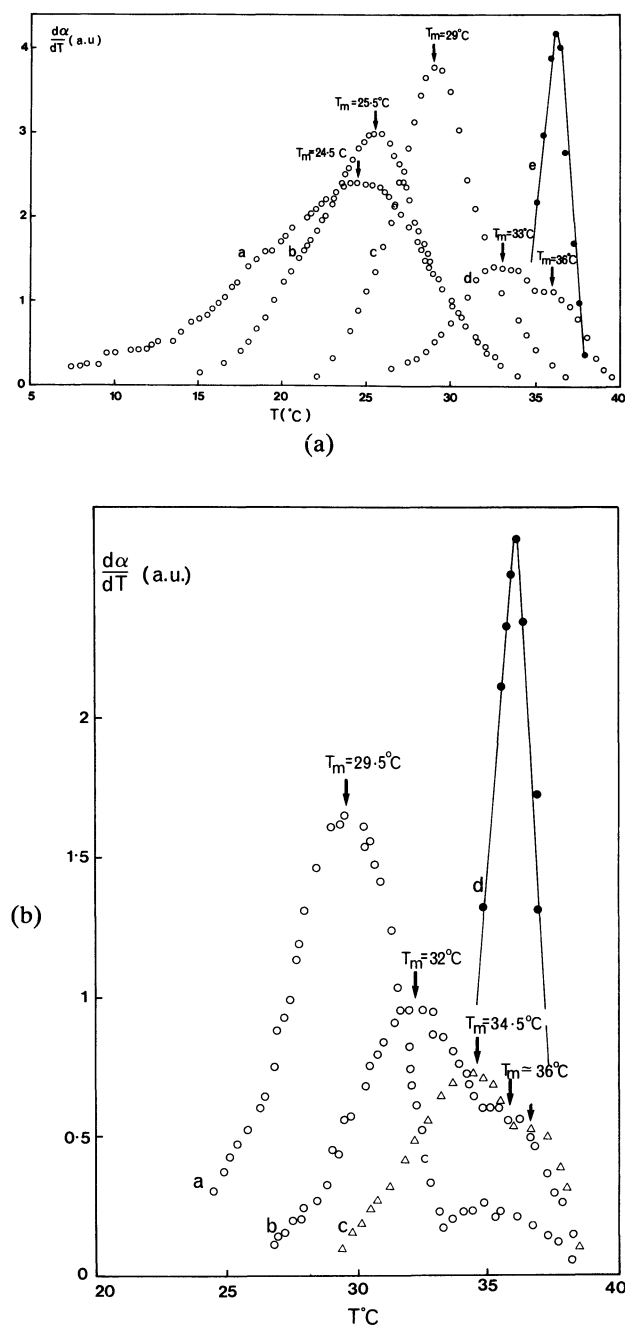


Fig. 6. — Melting peaks of gels matured at constant temperatures during 120 to 150 h. 6a) Concentration $c = 1\%$ g/g and different annealing temperatures: a) $T = 5^\circ\text{C}$, b) $T = 10.5^\circ\text{C}$, c) $T = 20.5^\circ\text{C}$, d) $T = 26.5^\circ\text{C}$, e) melting of a native collagen solution. 6b) Concentration $c = 4.7\%$ g/g and different annealing temperatures: a) $T = 22^\circ\text{C}$, b) $T = 26.5^\circ\text{C}$, c) $T = 28.2^\circ\text{C}$, d) collagen solution. for all measurements, $v = 0.05^\circ\text{C/min}$.

figure the results given by Godard *et al.* [8] obtained by DSC on gels of 5% g/g concentration, which were prepared by quenching and matured only for a short period (10-20 min). These results are very close to ours, which we did not expect; indeed, Godard *et al.* showed that during aging the melting temperatures of the gels increase progressively. A 3

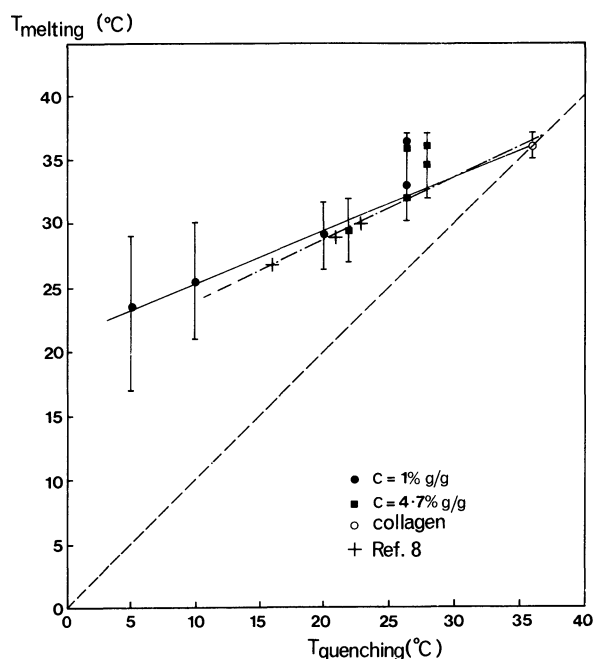


Fig. 7. — Melting temperatures T_m versus quenching temperatures T_q for two concentrations.

to 4°C shift should be observed after 150 h. The explanation may come from the high rates of heating used in DSC (2.5°C/min) which lead to an apparent shift of the melting curves towards high temperatures, or from differences in pH or ionic force of the solutions.

1.3 CONCLUSIONS FROM THE OPTICAL ROTATION MEASUREMENTS. — The optical rotation measurements allowed us to put clearly into evidence the influence of the thermal treatments on the microscopic structure of the gels. The helix amount reflects both the amount of renatured structure and its degree of stability (from the melting behaviour).

The helices formed have optical properties similar to the native collagen solutions but they have different thermal stabilities. The latter depends not only on the temperature at which the helices have been formed, but moreover significant variations exist between the helices grown in the same thermal conditions. A simple statement is that the more helices are formed, the less stable they are (at the same age and the same concentration). Several hypothesis can be made to explain the disorder of the structure :

- i) distribution of the length of the helical sequences,
- ii) local distortions of the angles and distances between atoms compared with their optimal values,
- iii) crystallization effects.

However, it is clearly observed that the collagen triple helix stability is the limiting value which the

gels reached after 150 h at concentrations of a few percent.

These observations corroborate those reported on the renaturation of dilute collagen solutions (0.1 to 0.4 % g/g), denatured just before by a mild heating [15-17].

The method of forming the gels by quenching and annealing at one temperature seems the best adapted for their systematic study. More complicated treatments such as repeated thermal cycles or alternate annealings, have also been reported in the literature [16]. Their analysis is more delicate, due to the mixing of time and temperature effects.

Besides the helix amount, other parameters have to be considered in order to understand the mechanisms of helix formation. We have investigated the role of the solvent by proton nuclear magnetic relaxation NMR. We have also visualized the supramolecular structure of the gels by developing ultra rapid freezing technics. These experiments are described in details elsewhere. Here, we shall recall the principal results.

2. Role of the solvent.

The role of the solvent in stabilizing the helical structures can be put into evidence by means of proton NMR.

As we explained in the section « Collagen and gelatin » water molecules are placed in interstitial positions and stabilize the triple helices of native collagen by establishing hydrogen bonds between adjacent chains. Also the polar groups such as OH, NH₂, CO... and the charged NH⁺ or COO⁻ groups, interact with water molecules in solution (coil conformation) by making hydrogen bonds or *via* dipolar interactions.

Thus, we expected to put into evidence a modification of the relaxation properties of water protons, in solutions and in gels, compared to the bulk water. The water molecules interacting with the protein should be sensitive to the change of conformation which transforms their microscopic environment.

The wide line NMR technique is unable to distinguish at « normal » temperatures (5 to 40 °C) different water populations : bound water and free water.

However, when the samples were cooled to temperatures below -8 °C, when part of the water freezes, then we could see that a fraction of protons still remains mobile [18]. These protons are partly those of the macromolecules and partly those of the bound water (water interacting with the protein). Our results, corroborating those obtained by other techniques on gelatin and collagen [19], gave an estimation of the fraction of bound water of 0.45 g/g of gelatin (which represents approximately 2.7 water molecules per amino acid residue).

By pulsed NMR, the spin-lattice relaxation time T_1 and the spin-spin relaxation time T_2 can be measured in solutions and gels. In both cases, single relaxation times were observed (exponential decays). This led us to the assumption that rapid exchange exists between the different water populations. The spin-lattice relaxation time is unaffected by the gelation phenomenon (helix formation). On the contrary, the spin-spin relaxation time T_2 is modified by the conformational changes. We observed a progressive decrease of T_2 during the quenching experiments, indicating that an increasing fraction of protons is involved into a rigid structure (see Fig. 8). We called this fraction the structural water. Within the assumption of a rapid exchange between various proton populations the inverse of the observed relaxation time T_2 is proportional to the fraction of structural water. Indeed, we showed that T_2^{-1} is proportional to the helix amount χ , measured by polarimetry. The fraction of structural water is thus related to the helix amount in the gel. Our theoretical interpretation of the NMR data is compatible with the models of triple helix stabilization by hydrogen bonds *via* water molecules which we mentioned at the beginning.

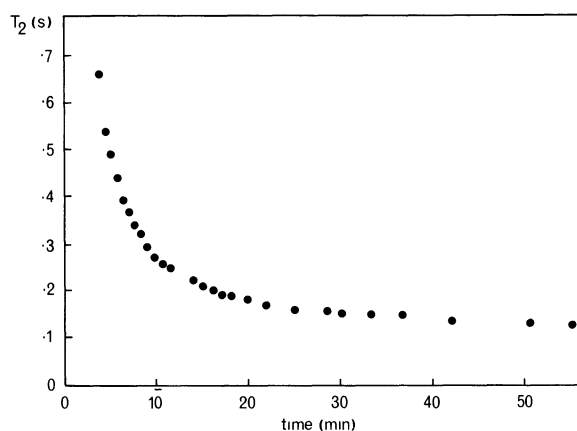


Fig. 8. — Decrease of the proton spin-spin relaxation time T_2 versus time during a quenching experiment ($c = 21$ % g/g, quenching temperature $T = 24$ °C) (from Ref. [18]).

3. The three dimensional structure.

Interpretations of the mechanical properties of polymer gels are invariably based on the assumption of a three dimensional connected network which extends throughout the solution. Also the ability of gels to hold a substantial amount of solvent (up to 99 %) is strongly related to their microstructure. The size of the pores has a direct influence on the capillary

forces which are especially strong for the smallest pores (range of 1-100 nm). A direct observation of the structure of the network is thus of primary importance. Moreover, a quantitative estimation of the parameters (for different concentrations or temperatures) might also help in elucidating the mechanisms of network growth.

So far, little information has been known about the three dimensional structure of physical gels.

Only recently, very performant techniques derived from advanced methods of electron microscopy, developed by researchers in Life Sciences, became available. The difficulties in performing electron micrographs of the gels are similar to those encountered in most biological specimens. First of all, comes the lack of contrast: the atomic numbers along the macromolecules are not high enough to scatter electrons. Traditionally, staining methods have been applied [30], using solutions containing heavy atoms to create the contrast. These methods usually include chemical fixing of the specimen and embedding with epoxy resins.

When studying physical gels, like gelatin, other major difficulties come from the high degree of hydration and from the weakness of the bonds which hold the network. The physical networks therefore, have to be « locked » by chemical crosslinks or fixed by a physical method. In the latter case, quick freezing techniques are used.

Their application to electron microscopy became possible only when ultrarapid rates of cooling could be achieved in order to avoid crystallization of water [20]. The growth of ice crystals damages the structure (of cells, tissues, etc.). The crystal size is mainly a function of the freezing rate. The vitreous state of water can be attained for rates of cooling of the order of 10^5 K sec^{-1} [21]. We have adapted a method of quick freezing [22] by using a device first designed and built by Escaig [23] and tested on biological specimens. The device is commercially available from Reichert-Young (the cryoblock). In practice, the gel is layed on a sample holder and an electropneumatic system pushes it against a copper block which was previously cooled with liquid Helium down to about 10 K. Over a depth of $10 \mu\text{m}$ from the surface of the gel, the rate of cooling reaches 2×10^4 to $3 \times 10^4 \text{ K sec}^{-1}$. Ice crystals cannot be detected in this range, which means either that water is actually vitrified or, if any ice crystals are formed, their size is beyond the resolution of electron micrographs (a few angströms). In this range, the network is preserved. After freezing, the sample is stored in liquid nitrogen, then mounted in a Balzers equipment where the freeze etching is done. As the sample is kept at -100°C under vacuum, the vitreous ice is sublimated over a depth of $0.5 \mu\text{m}$. The polymeric network becomes apparent. The replica of the structure is realized by evaporating

Pt and C (rotatory shadowing). The coating stiffens the structures and it is not altered by the electron beam. The organic material remaining is removed by acid treatment. The replica is layed on a microscopic grid and observed.

We realized [24] replicas of dilute hot solutions and gels of concentrations $\leq 1 \text{ \% g/g}$. We present in figure 9 the replica of a 0.5 \% g/g gelatin gel which was formed at room temperature and kept for two weeks. Even at this low concentration, a dense network is seen. Linear filaments randomly oriented delimit meshes of variable sizes. The filaments thickness is mainly due to the coating (5-10 nm) which was too much abundant in this case. Stereoscopic images of the replicas can be taken. They allow to separate different heights of the image providing a three dimensional image of the network.



Fig. 9. — Replica of a gelatin gel of concentration $c = 0.5 \text{ \% g/g}$ formed at room temperature during two weeks. The bar indicates $0.5 \mu\text{m}$.

Further work is underway to optimize the method of replication and to derive a quantitative analysis of the network parameters.

The disordered nature of the network is clearly shown by the replicas.

4. Theoretical interpretation.

We start with the phenomenological analysis of the kinetics of helix growth and discuss the possible interpretations of the data. Then we present a simple microscopic model which can account for the main structural features which were observed. The model can be improved when more informations of the network will be known.

4.1 PHENOMENOLOGICAL ANALYSIS. — We first refer to the data given in figure 4. In order to analyse

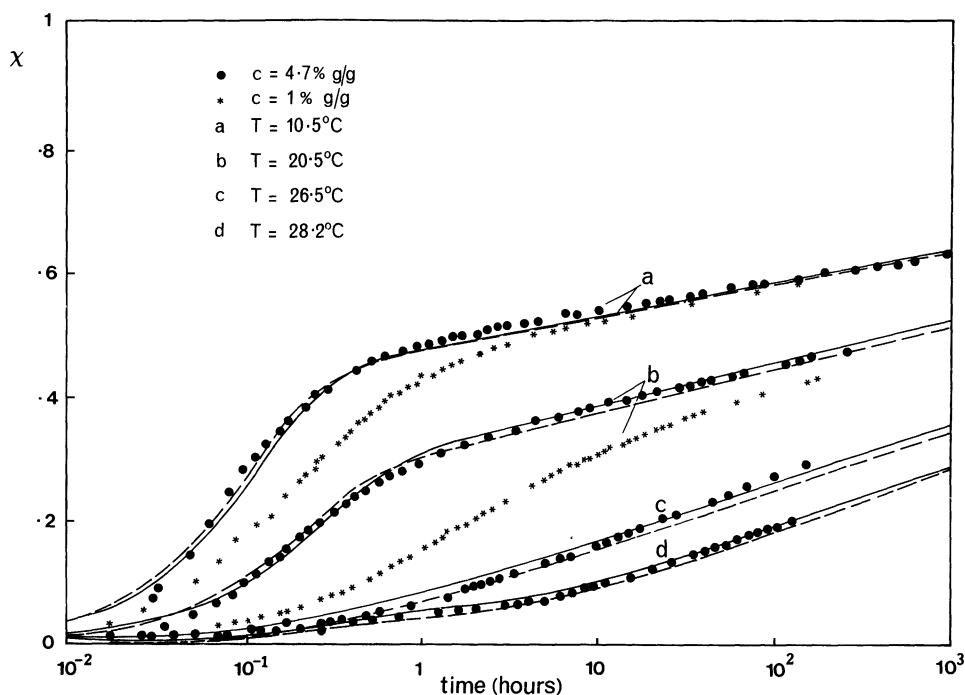


Fig. 10. — Increase of the helix amount as a function of time, in logarithmic scale (concentrations and temperatures as indicated). The continuous lines are calculated using equation (4), the dashed lines, using equation (5).

the kinetics at short time scale and at long term, we plot in figure 10 the helix amount as a function of time, in hours, in a logarithmic scale. For different temperatures of gelation, the overall kinetics can be decomposed in two processes : the rapid one and the slow one.

4.1.1 The rapid process. — An exponential time dependence of the helix amount is observed during the first minutes of a quenching experiment. This can be seen in figure 11: by plotting $\log[-\log(1-\chi)]$ versus $\log t$ a linear plot is obtained between 2 and 5 or 7 min after the beginning of the quenching which is quite a short period. This period is delimited on one side by the time for temperature equilibration of the sample (the first one or two minutes) and on the other side by the development of the second process which we called the slow process. This first, exponential step, of the helix growth has been observed on various samples of gelatin, by different methods such as DSC [8], ultrasonic absorption [25] and again optical rotation [25].

4.1.2 The slow process. — In the plot of figure 10, one can see that the growth of helices proceeds more and more slowly, at a logarithmic rate. We have followed this process over a period of 1 000 h, for one of the samples ($T = 10^\circ\text{C}$, $c = 4.7\% \text{ g/g}$) and we didn't observe a limiting value for the helix amount. The logarithmic process is slower at the lower temperatures.

Here again, such effects have been reported for

various samples of gelatin and also for the renaturation of collagen single chains in dilute solutions [15].

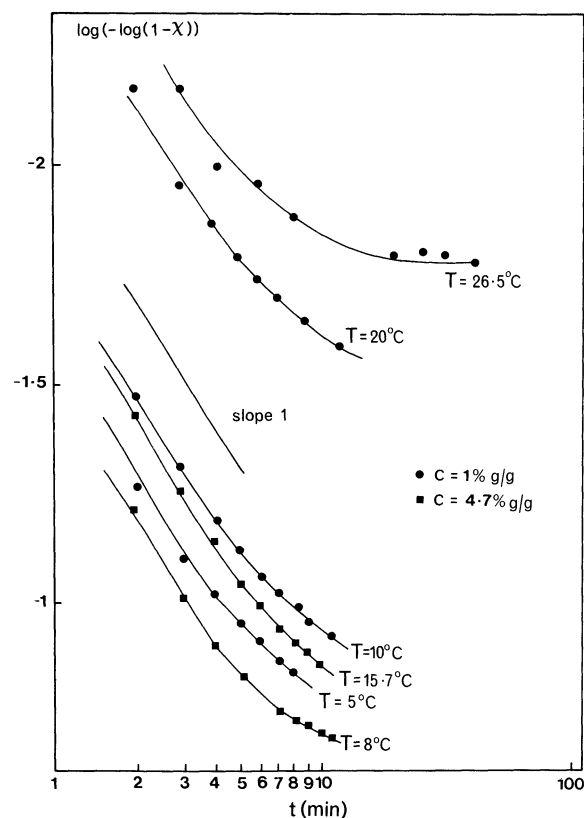


Fig. 11. — Time dependence of the rapid process indicating an exponential increase of the helix amount.

4.1.3 Formal kinetics. — We propose [14] a formal analysis of the kinetics by choosing two different hypothesis.

i) The two mechanisms are independent. So, one can write the total helix amount $\chi(T, t)$ as the sum of two terms :

$$\chi(t, T) = \chi_0(T) \left\{ 1 - \exp \left(-\frac{t}{t_F} \right) \right\} + \chi_1(T) \text{Log} \left(\frac{t}{t_S} + 1 \right). \quad (4)$$

$\chi_0(T)$ is the amplitude of the first process, t_F is the characteristic time (fast process), $\chi_1(T)$ defines the slope of the second process as a function of the logarithm of time, t_S is the characteristic time for the second process (slow process) to appear.

ii) The two mechanisms are not independent : the second process realizes the annealing of the helices created during the first one. Then :

$$\chi(t, T) = \int_0^t \frac{d}{dt'} \left(1 - \exp \left(-\frac{t'}{t_F} \right) \right) \times \left[\chi_0(T) + \chi_1(T) \cdot \text{Log} \left(\frac{t - t'}{t_S} + 1 \right) \right] dt'. \quad (5)$$

During a time interval dt' , helices are created by the first process. The rate of formation is given by the derivative of $\left[1 - \exp \left(-\frac{t'}{t_F} \right) \right]$. The amplitude of this process is $\chi_0(T)$. Then annealing starts, with a time origin t' , a slope in a logarithmic time scale given by $\chi_1(T)$ and a characteristic effective time t_S .

So, at a moment t , the helices present are those at the native state (first process) and those created by annealing during the time intervals $(t - t')$. We have integrated over time between $0 \leq t' \leq t$.

Both fits are given in figure 10 for $c = 4.7$ % g/g. The solid line refers to equation (4) ; the broken line, to equation (5). The numerical values of the parameters are given in reference [14], table I. Both fits are in a good agreement with the measurements. The numerical values for t_F are close to those derived from the plot in figure 11. The amplitude $\chi_0(T)$ of the first mechanism varies strongly with temperature : 40 % at 10 °C to 4 % at 28 °C. The time t_S increases with temperature : from 2 min at 10 °C to 4 h at 28 °C. Both equations (4) and (5) give similar values for these parameters.

4.1.4 Discussion. — The formal analysis of the kinetics of helix growth did not give a clear indication of the nature of the mechanisms involved in the helices formation. We have established that, formally, the kinetics can be analysed as the sum of two processes, which are either independent or related to each other.

The first mechanism is exponential in time. It has been interpreted by Godard *et al.* [8] as typical of a crystallization phenomenon. Indeed, these authors applied a formalism which is familiar to metallurgists and physicists working in the field of polymer crystallization. In general, the volume fraction, X , of transformed (crystallized) material is a function of time, of the type :

$$X(t) = 1 - \exp^{-Kt^n} \quad (6)$$

K is the equivalent of a reaction constant and depends on the temperature ; n is called the Avrami exponent. Depending on the geometrical shape of the crystallites and the nature of the nucleation mechanism, different values for n can be predicted. Actually, the value $n = 1$ corresponds to an athermal nucleation of fibers : a fixed number of sites nucleate fibers, of constant diameter, which grow unidirectionally.

So, such fibers would be nucleated from the very beginning of the process. Their diameters have been calculated, as depending on the temperature of gelation and concentration. According to the nucleation theories the larger diameters of the nuclei correspond to the higher temperature of crystallization.

This interpretation supposes also that the extrapolated melting temperature of fully developed crystals departs from the melting temperature of a single triple-helix as the association of helices through fibers provides a mutual additional, stabilization [29, 31]. Our measurements, based on gels annealed for a longtime, show that the network has a thermal stability which is, at best, comparable to the collagen triple helix. Also the structure of the gels, as observed by electron microscopy, does not reveal the striated image, typically due to the regular shift of 67 nm of the collagen rods in the fibrils of native tissues. Therefore, such fibrils are not renatured in gels.

Finally, by careful rheological measurements, that we report in the next paper, we found that the elastic moduli of the gels, during the beginning of gelation, are independent of the temperature, in the range $24 < T < 28$ °C ($c = 5$ % g/g). The moduli are uniquely related to the helix amount χ , for $\chi < 15$ %. This suggests that the structures nucleated at the different temperatures are almost identical. If the nuclei of crystallization had diameters depending on the temperature, one would expect a marked temperature dependence of the elastic moduli.

All these arguments led us to the conclusion that the mechanism of helix renaturation is a conformational transformation which induces a three-chain association. Starting with this statement, several alternatives can be chosen to explain the mechanisms of network growth.

In this paper, we propose an interpretation of the

data which we do not consider as a definitive model for the gelatin gel network, but which accounts for the main features reported here. Further experimental work is under way which will describe the network more precisely and will help to refine the model.

4.2 ATTEMPT FOR A MICROSCOPIC INTERPRETATION. — The scheme that we propose for semidilute solutions is the following: when the temperature is lowered, helices are nucleated along the individual chains. For instance, sequences containing Proline residues provide potential sites of nucleation [12]. If helices are nucleated on segments belonging to three different chains which are closely entangled then a triple helix is able to start and grow. Assuming that one chain is involved in several — at least two — of these junctions, then a loose network is created. This mechanism might correspond to the first rapid process of helix growth. The second process should then be a slow reorganization of the network towards the collagen rods renaturation.

i) *Loose network growth.* — We consider a solution of independent, flexible chains of N units. We make the hypothesis that each chain has nucleated two helical sequences which represent the junctions of the network (see Fig. 12a). The two junctions are separated by a distance r , which depends on the local concentration in solution (contacts between three chains). We take r as a fixed parameter.

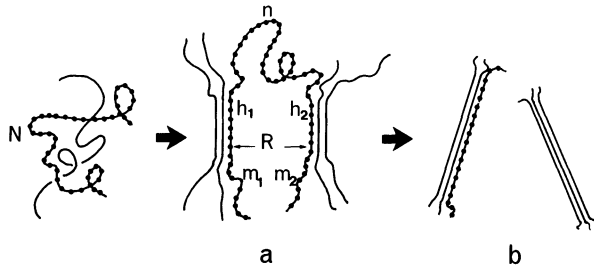


Fig. 12. — The two steps involved in the gelation process: a) formation of a loose network, b) equilibrium configuration (renaturated collagen solution).

By using simple statistical mechanics, one can calculate the helix amount corresponding to the equilibrium of this configuration.

So, one unit of the chain can either be in a coil or in a helix conformation. Let n be the number of units forming the coil between the junctions, h be the total number of units in helical conformation, m be the total number of units at the free ends of the chain. For both junctions (1) and (2), one has:

$$\begin{aligned} h &= h_1 + h_2 \\ m &= m_1 + m_2 \\ N &= m + h + n. \end{aligned} \quad (7)$$

We assign a binding energy ε to one unit in the helical state. ε is the energy necessary to transform one unit from coil to helix ($\varepsilon < 0$). The probability f for a chain, at the temperature T , to have h units in the helical conformation, is given by:

$$f(N, r, T, h) \sim \Omega e^{-\varepsilon h/kT} \quad (8)$$

Ω is the total number of microscopic configurations, k is the Boltzmann constant.

The thermodynamic weight Ω' of a coil of n units, with an end to end distance r is given by [26]:

$$\text{Log } \Omega'(r, n, T) = n \left[C + \text{Log } \frac{\sin hx}{x} - xX \right]$$

with the following notations:

$$X = \frac{r}{na}; \quad x = \frac{Fa}{kT} \quad (9)$$

$$X = \mathfrak{L}(x) = \coth x - \frac{1}{x} \quad (10)$$

$\mathfrak{L}(x)$ is the Langevin function, a is the length of one polymer unit in coil conformation, F is the force exerted at both ends of the coil bridging between junctions to maintain the distance r , C is a constant which can be calculated from the number of configurations of a free chain of n units:

$$\text{Log } C \simeq (4\pi)^n. \quad (11)$$

Therefore:

$$\Omega'(n, r, T) \simeq (4\pi)^n e^{-Xxn} \left(\frac{\sin hx}{x} \right)^n. \quad (12)$$

If no minimum length is required for a helical sequence, then there are h possibilities to share the h helical units between two junctions; $N - h - n$ possibilities for the free end units and $(4\pi)^{N-h-n}$ configurations for them.

This allows us to calculate Ω :

$$\begin{aligned} \Omega &\simeq \sum_{n=r/a}^{N-h} (4\pi)^{N-h} h(N-h-n) \times \\ &\quad \times \left(\frac{\sin hx}{x} \right)^n e^{-Xxn} \end{aligned} \quad (13)$$

$n = r/a$ corresponds to the coil completely stretched, $n = N - h$ when no free ends are left.

The equilibrium value for h maximizes the probability $f(h)$, for a given set of the parameters:

$$R = \frac{r}{a}; \quad T_0 = \frac{|\varepsilon|}{k} \quad \text{and} \quad N.$$

We made the assumption of a Gaussian chain conformation ($n \gg \frac{r}{a}$) and computed $f(h)$ from $n = N - h - 100$ to $n = N - h$. As three residues are needed to make a turn of the left-handed helix, we assume that one unit is three residues. Thus, as a

chain has 1 000 residues, N is of the order of 400 units. Let χ_0 be the helix amount given by :

$$\chi_0 = \frac{h(\max)}{N} \quad (14)$$

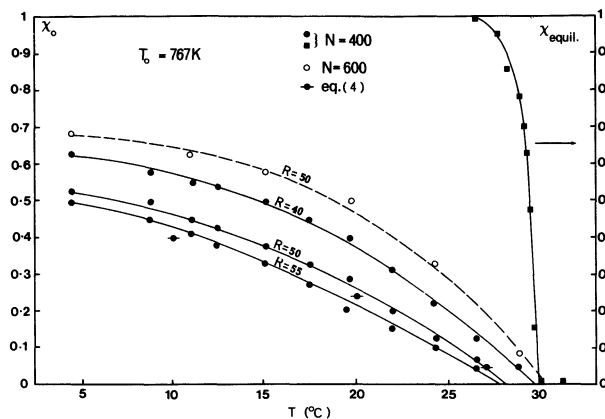


Fig. 13. — Computed values of the helix amounts *versus* temperature. The influence of the chain length N and of the distance R between junctions is shown. χ_0 represents the helix amount at the end of the first process. χ_{equil} represents the hypothetical values reached if the second process could arrive to completion. χ_0 corresponds to the maximum of $f(h)$ (Eq. (8)), χ_{eq} to the maximum of $f'(h)$ (Eq. (15)).

$h(\max)$ corresponds to the maximum of the computed probability $f(h)_{\max}$.

We plot in figure 13, χ_0 as a function of temperature taking :

$T_0 = 767$ K ; $N = 400$; $R = 40$, or $R = 50$, or $R = 55$ as well as $N = 600$ and $R = 50$, same T_0 .

The length of a unit of three residues being around 0.9 nm, r is comprised between 40 and 50 nm.

The values of χ_0 derived from equation (14) are also reported in figure 13. They are in agreement with this model when $R = 50$ ($r \approx 45$ nm), $N = 400$ and $T_0 = 767$ K. The corresponding binding energy, per mole is then :

$$|\varepsilon(\text{mole})| = 1.5 \text{ kcal/mole}.$$

It has the order of magnitude of the hydrogen bond. The numerical values for N , R , ε have to be considered as averages ; a large distribution is revealed by the melting behaviour, the molecular weight analysis, etc... However, these values are in a reasonable agreement with the structural and thermodynamical data which is known.

When this first step is achieved, the system is not truly in equilibrium. A second process reorganizes the network and allows new helices to be created. The second process has a logarithmic time dependence, which is much slower than the first one. There is not at the moment a theoretical model

which can explain the logarithmic process. It might represent a superposition of several mechanisms, having a distribution of the characteristic times. An analogy with the glass relaxation can be suggested [27].

We may suppose that during this process local constraints are released.

ii) *Equilibrium configuration.* — If the second process could arrive to completion one chain would free itself from one junction and form a continuous helical sequence on the other one. The final equilibrium would then correspond to independent triple helices, like the native collagen rods in solution.

In this configuration (see Fig. 12b), one can compute the most probable value χ_{equil} as a function of temperature, for a chain of N units, by searching the maximum of :

$$f'(h, T, N) \sim (4\pi)^{N-b} (N-h) e^{-\varepsilon h/kT}. \quad (15)$$

The numerical values of χ_{equil} are also reported in figure 13, keeping the same data for N and T_0 as in the precedent section ($N = 400$, $T_0 = 767$ K).

The plot of $\chi_{\text{equil}}(T)$ is similar to a step melting curve such as :

$$\begin{aligned} \chi_{\text{equil}} &= 1 & T < 26.5^\circ \text{C} \\ \chi_{\text{equil}} &= 0 & T \geq 30^\circ \text{C}. \end{aligned}$$

Although the system proceeds towards this state, the final equilibrium is not reached within the longest periods of observation.

Conclusion.

The aim of this paper is to make a statement on different aspects involved in the structural modifications of gelatin solutions, during gelation. We stressed upon the influence of thermal treatments, on solutions of various concentrations. We clearly establish that the gel state is not an equilibrium state. The kinetic aspects have to be considered. Although different interpretations of the kinetics have been proposed, we argue that the conformational transition of the protein chains is the predominant mechanism of gelation.

Several features appear through this investigation which can be generalized to other physical gels :

1) Gels have to be characterized at several microscopic levels, starting from the local conformation (a few tenths of nanometers) to the overall three dimensional organization, in ranges of several hundreds of nanometers. The full scale is important to understand the mechanisms of gelation and to explain the elastic properties of the gels and their remarkable ability of holding large amounts of solvent. The observation by electron microscopy of the three dimensional structure of gels is now possible. We propose a freeze etching and replication

method which is suitable for dilute gels ($c = 1$ to 2% g/g).

2) In connection with the ability of gels to hold the solvent, we know, first, that significant amounts of loosely bound water exist, in solution. We have established, for aqueous gelatin solutions, that water participates to the built up of the network (tightly bound, structural water). Although such properties

are to be expected in aqueous systems, similar effects have been reported recently for physical gels of synthetic polymers, in apolar solvents (formation of polymer solvent complexes for atactic polystyrene in carbon disulfide [28]). Such observations are encouraging for the search of a general description of the physical gelation.

References

- [1] *Treatise on collagen*, Ramachandran G. N. Ed. (N.Y. Acad. Press) 1967.
- [2] WARD, A. G. and COURTS, A., *The science and technology of gelatin* (Acad. Press) 1977.
- [3] EYRE, D. R., *Sciences* **207** (1980) 1317.
- [4] BROWN, F. R., HOPFINGER, A. J. and BLOUT, E. R., *J. Mol. Biol.* **63** (1972) 101.
- [5] RAMACHANDRAN, G. N. and CHANDRASEKHARAN, R., *Biopolymers* **6** (1968) 1649.
- [6] BOEDKER, K. and DOTY, P., *J. Phys. Chem.* **58** (1954) 968.
- [7] HARRINGTON, W. F. and RAO, N. V., *Biochem.* **9** (1970) 3714.
- [8] GODARD, P., BIEBUYCK, J. J., DAUMERIE, M., NAVEAU, H., MERCIER, J. P., *J. Polym. Sci., Polym. Phys. Ed.* **16** (1978) 1817.
- [9] DJABOUROV, M. and PAPON, P., *Polymer* **24** (1983) 539.
- [10] WALTON, A. G. and BLACKWELL, J., *Biopolymers* (Acad. Press) 1973.
- [11] BLOUT, E. R., CARVER, J. P., GROSS, J., *J. Am. Chem. Soc.* **85** (1963) 644.
- [12] VON HIPPEL, P. H., reference [1], chap. VI.
- [13] VON HIPPEL, P. H. and WONG, K. Y., *Biochem.* **2** (1963) 1399.
- [14] DJABOUROV, M., MAQUET, J., THEVENEAU, H., LEBLOND, J., PAPON, P., *Br. Polym. J.* **17** (1985) 169.
- [15] BEIER, G. and ENGEL, J., *Biochem.* **5** (1966) 2744.
- [16] KUHN, K., ENGEL, J., ZIMMERMANN, B., GRASSMANN, W., *Arch. Biochem. Biophys.* **105** (1964) 387.
- [17] KUHN, K., ZIMMERMANN, B., *Arch. Biochem. Biophys.* **109** (1965) 543.
- [18] MAQUET, J., THEVENEAU, H., DJABOUROV, M., LEBLOND, J., PAPON, P., *Polymer* **27** (1986) 1103.
- [19] MREVLISHVILI, G. M., SHARIMANOV, Yu. G., *Biofiz.* **23** (1978) 242.
- [20] *Freeze etching techniques and applications*, Benedetti, E. L. and Favard, P., Ed. (Soc. Franç. Microsc. Electron., Paris) 1973.
- [21] GILKEY, J. C. and STRAEHELIN, L. A., *J. Electron. Microsc. Technol.* **3** (1986) 177.
- [22] HEUSER, J., *J. Cell. Biol.* **79** (1978) 224a.
- [23] ESCAIG, J., *J. Microsc.* **126** (1982) 221.
- [24] FAVARD, P., FAVARD, N., DJABOUROV, M., LEBLOND, J., to be published.
- [25] EMERY, J., CHATELIER, J. Y., DURAND, D., *J. Phys. France* **47** (1986) 921 and related papers.
- [26] FLORY, P., *Principles of polymer chemistry* (Cornell Univ. Press, N.Y.) 1953.
- [27] MEIJER, P. H. E., private communication.
- [28] FRANÇOIS, J., GAN, J. Y. S., GUENET, J. M., *Macromolecules* **19** (1986) 2755 and related papers.
- [29] FLORY, P. and GARRETT, R. R., *J. Am. Chem. Soc.* **80** (1958) 4836.
- [30] TOMKA, I., BOHONEK, J., SPÜHLER, A. and RIBEAND, M., *J. Photogr. Sci.* **23** (1975) 97.
- [31] BORCHARD, W., BREMER, W., KEESE, A., *Colloid Polym. Sci.* **258** (1980) 516.